Theor Chim Acta (1987) 72: 57-62

Theoretica Chimica Acta

Topological properties of the electronic density of CO–MgF_2 and OC–MgF_2 adducts

O. G. Stradella,[1] S. A. Maluendes,[1] E. A. Castro, and A. H. Jubert[2]

[1] División Química Teórica, INIFTA, Sucursal 4, CC 16, 1900 La Plata, Argentina
[2] Cátedra de Química Inorgánica, Facultad de Ciencias Exactas, Universidad Nacional de La Plata, 47 y 115, 1900 La Plata, Argentina

(Received November 27, 1986, revised March 10, Accepted March 13, 1987)

By means of Bader's approach on topological properties of the electronic density, the major stability of the O-bonded adduct over the C-bonded one between MgF_2 and CO is reinforced.

Key words: Quantum topology — *Ab-initio* MO calculations — Linkage CO isomers

1. Introduction

In a previous paper *ab-initio* MO calculations were performed on the C- and O-bonded adducts of MgF_2 with CO using different basis sets [1]. In all cases, the O-bonded isomer was found to be more stable than the C-bonded one. Mulliken's population analysis indicates that the Mg–O interaction is mainly ionic as expected from Klopman's theory [2].

One interesting approach for the analysis of bonds and intermolecular interactions is that provided by the quantum topology of the electronic density. This theory was developed by Bader and co-workers [3, 4] and it is based on the fact that the distribution of the electronic charge in a molecular system determines its structural characteristics.

The aim of this work is to assess our previous results [1] by means of Bader's approach on the major stability of the O- linkage isomer.

Before discussing our results we will sketch the relevant properties of the quantum topology of the electronic density.

2. Theory

The theory makes a subdivision of the real space in non overlapping subspaces Ω corresponding to atoms in a molecule. The criterion used to make the partition is that the atomic regions must be separated by zero-flux surfaces $S(\boldsymbol{r})$ defined by

$$\nabla\rho(\boldsymbol{r}) \cdot \boldsymbol{n}(\boldsymbol{r}) = 0, \quad \boldsymbol{r}/\varepsilon/S(\boldsymbol{r}) \tag{1}$$

where $\rho(\boldsymbol{r})$ is the one-electron density distribution and $\boldsymbol{n}(\boldsymbol{r})$ the unit vector normal to the surface S. For all surface points the flux of $\nabla\rho(\boldsymbol{r})$ vanishes. The choice of this criterion is found on the topological features of $\rho(\boldsymbol{r})$ [3–5] and on the evidence obtained from the analysis of computed molecular densities $\rho(\boldsymbol{r})$ and their associated gradient vector field $\nabla\rho(\boldsymbol{r})$ [6]. Besides it has been shown that all properties of a subspace Ω are quantum mechanically defined in the same way as for the total molecular system [4–5].

The zero-flux surfaces pass through a point where $\nabla\rho\ (\boldsymbol{r}_c) = 0$ ($\boldsymbol{r}_c$ being a critical point). All the critical points of $\rho(\boldsymbol{r})$ have a structural meaning [7]. The properties of a critical point are determined by the eigenvalues of the Hessian matrix of $\rho(\boldsymbol{r})$, $H_{ij} = [\partial^2\rho(\boldsymbol{r})/\partial x_i\, \partial x_j]_{\boldsymbol{r}=\boldsymbol{r}_c}$. The eigenvectors associated with the eigenvalues determine gradient paths which either terminate or originate at the critical point if the eigenvalue is negative or positive respectively. For critical points of rank (number of non zero eigenvalues) three, only four values for the signature (number of excess positive over negative eigenvalues) are possible: +3, +1, −1, −3. A (3, −3) critical point is a maximum in $\rho(\boldsymbol{r})$ and they are found almost without exception only over the nuclear positions. The critical points of signature +1 or −1 are saddle points. A (3, −1) saddle point has a positive eigenvalue and its associated eigenvector gives origen to two oppositely directed gradient paths which define a unique axis in space along which $\rho(\boldsymbol{r})$ increases for motion away from the critical point reaching its maximum value at (3, −3) critical points. The gradient paths generated by the two eigenvectors corresponding to the negative eigenvalues define the aforementioned zero-flux surface. Motion in this surface in any direction away from the critical point leads to a decrease in $\rho(\boldsymbol{r})$. Because of these characteristics the (3, −1) critical point has been called the bond critical point and the gradient path which links it to the two adjacent nuclei is known as the bond path. The remaining types of critical point may be shown to be associated to ring and cages structures ((3, +1) and (3, +3), respectively).

The value of $\rho(\boldsymbol{r}_b)$, being $\boldsymbol{r}_b$ a bond critical point, is characteristic of the bind of bond [6a].

An important property of $\rho(\boldsymbol{r}_b)$ is the ratio λ_1/λ_2 of its negative curvatures along axes perpendicular to the bond path. The ellipticity $\varepsilon = (\lambda_1/\lambda_2) - 1$ provides a quantitative generalization of the $\sigma - \P$ character of a bond [6a]. In a simple way we may state that for a simple bond the radial distribution of $\rho(\boldsymbol{r})$ along the bond path is uniform, so that $\varepsilon = 0$. For a double bond the contours of $\rho(\mathbf{r})$ in the interatomic surface around $\boldsymbol{r}_b$ are elliptical in shape hence λ_1 and λ_2 are different and their associated eigenvectors define a pair of orthogonal axes perpendicular to the bond path: the minor axis along which the magnitude of

the negative curvature or $\rho(\mathbf{r})$ is a maximum (λ_1) and the major axis along which its magnitude is a minimum (λ_2), $\lambda_1 > \lambda_2$. Finally for a triple bond, again $\lambda_1 = \lambda_2$ and $\varepsilon = 0$. The existence of a ¶ delocalization of electrons from one bond to another may be detected by a decrease in $\rho(r_b)$ or the bond order and a corresponding increase for the other bond, compared with cases of known conjugation, and by a parallelism between the major (and minor) axes of the two bonds.

When studying a bond from the energetical point of view, the kinetic energy density may be defined as

$$G(\boldsymbol{r}) = \tfrac{1}{2}\nabla\nabla'\Gamma'(\boldsymbol{r}, \boldsymbol{r}')_{r=r'} \tag{3}$$

where Γ' is the one electron density matrix [8]. This kinetic energy density can be related to the local potential energy density $V(\boldsymbol{r})$ [9].

$$2G(\boldsymbol{r}) + V(\boldsymbol{r}) = \tfrac{1}{4}\nabla^2\rho(\boldsymbol{r}) \tag{4}$$

$$V(\boldsymbol{r}) = N\int d\tau' [\Psi^*(-\boldsymbol{r}\nabla(\hat{\mathcal{V}})\Psi], \tag{5}$$

where $d\tau'$ denotes the spin coordinates of all N electrons and the cartesian coordinates of all N electrons but one, and $\hat{\mathcal{V}}$ is the quantum mechanical potential operator. The Langrangian density $L(\boldsymbol{r}) = -\frac{1}{4}\nabla^2\rho(\boldsymbol{r})$ is a good measure of the concentration of charge density [10]. If the Langrangian density in a point is positive then the charge density is concentrated in that point and if negative it is depleted.

The molecular energy density $H(\boldsymbol{r})$ is related to $G(\boldsymbol{r})$ and $V(\boldsymbol{r})$ by

$$H(\boldsymbol{r}) = G(\boldsymbol{r}) + V(\boldsymbol{r})$$

since $G(\boldsymbol{r})$ is always positive and $V(\boldsymbol{r})$ is always negative, the sign of $H(\mathbf{r})$ reveals whether $V(\boldsymbol{r})$ or $G(\boldsymbol{r})$ dominates in the bonding region. A dominance of $V(\mathbf{r})$ indicates that accumulation of charge is stabilizing in that region. On the other hand, if $G(\boldsymbol{r})$ dominates then the concentration of charge is destabilizing. For covalent bonds $H(\boldsymbol{r}) < 0$ and $L(\boldsymbol{r}) > 0$ in the bonding region (in particular in the bond critical point). For ionic bonds (non covalent closed shell interactions) $H(\boldsymbol{r}) > 0$ and $L(\boldsymbol{r}) < 0$.

3. Analysis of results

In this section we will discuss the topological properties of the electronic density, which are summarized in Tables 1 and 2, for the O-Mg and C-Mg interactions calculated with 6-31G basis set. The conclusions that will be shown are also valid when using different basis sets.

In Table 1 we show the charge (ρ), kinetic energy (G), potential energy (V), electronic energy (H) densities, the laplacian of the charge density ($\nabla^2\rho$) and the ellipticity for each bond critical point. We include the data for the isolated

Table 1. Topological properties of the electronic density for O-Mg, C-Mg, C=O, within both adducts and the isolated C≡O molecule [au]

	$CO-MgF_2$		$OC-MgF_2$		
	O-Mg	C=O	C-Mg	C=O	C≡O
$\rho(r_b)$	0.0237	0.4296	0.0166	0.4632	0.4484
$\nabla^2\rho(r_b)$	0.2170	0.8566	0.1127	0.8641	0.8413
$G(r_b)$	0.0422	0.8642	0.0222	0.9581	0.9133
$V(r_b)$	−0.0301	−1.1543	−0.0161	−1.7000	−1.6163
$H(r_b)$	0.0121	−0.6500	0.0060	−0.7420	−0.7029
ε	0.0255	0.0045	0.0890	0.0030	0.0000

Table 2. Eigenvalues and eigenvectors of the Hessian at the critical point in O-Mg, C-Mg and C=O within both adducts

	O-Mg			C=O		
	λ_1	λ_2	λ_3	λ_1	λ_2	λ_3
	−0.0362	−0.0353	0.2886	−1.4843	−1.4776	3.8184
x	0.0148	0.4894	0.8719	0.0000	−0.5000	0.8666
y	−0.9996	0.2820	0.0012	1.0000	0.0000	0.0000
z	−0.0240	−0.8716	0.4897	0.0000	0.8660	0.5000

	C-Mg			C=O		
	λ_1	λ_2	λ_3	λ_1	λ_2	λ_3
	−0.0208	−0.0191	0.1526	−1.5574	−1.5527	3.9743
x	0.0163	0.4809	0.8766	−0.4999	0.0000	0.8660
y	−0.9996	0.0292	0.0026	0.0000	1.0000	0.0000
z	−0.0243	−0.8763	0.4811	0.8660	0.0000	0.4999

CO molecule. In Table 2 we display the eigenvalues and their associated eigenvectors for the ligand-metal and C-O bond critical points. The molecule is located in the x-z plane.

First of all $\rho(r_b)$ in the metal-ligand critical point is low in both isomers compared with the C≡O bond. The Langrangian density $L(\mathbf{r}_b)$ is negative and the electronic energy density $H(r_b)$ is slightly positive. All these features are characteristic of ionic interactions. Comparing the critical points of the two isomers $CO-MgF_2$(1) and $OC-MgF_2$ (2) the electronic charge density is greater in the former. The Langrangian density is lower in 1, so that in spite of the greater electronic density in 1 compared with 2 we conclude that in 1 is more depleted because it is more contracted in the internuclear axis direction (see also the magnitude of the positive eigenvalue). This suggests a greater ionicity of the CO-Mg interaction compared with the OC-Mg.

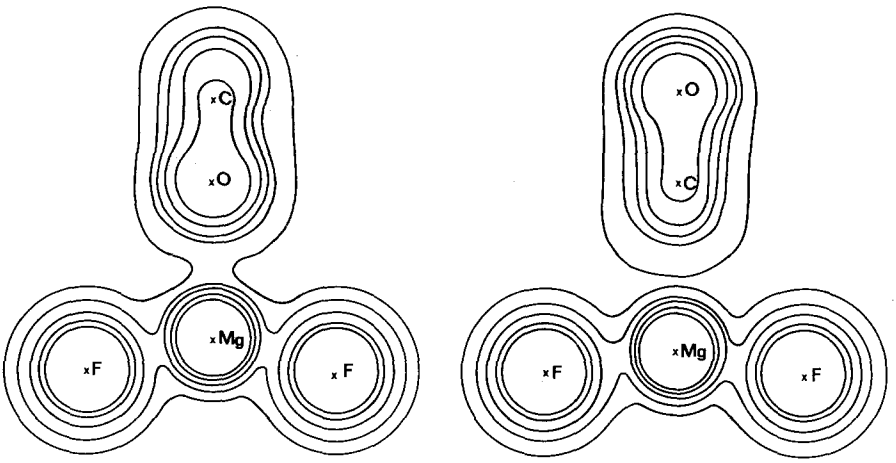

Fig. 1. Contour maps of the electronic charge distribution for the OC-MgF_2 and CO-MgF_2 adducts. Profiles values: 0.02. 0.06, 0.10, 0.18, 0.34

The origin of the greater electronic density in 1 (shown in Fig. 1 by means of a density map) may be traced back to the following facts: (a) The electronic density in the C=O critical point is greater in the isolated CO molecule compared with the CO-MgF_2 by 4.3% but lower compared with the OC-MgF_2 by 3.2%; they are minor differences (density in C=O bond critical point is lower than C=O density by 16%) but nevertheless important to our discussion; (b) The CO bond critical point in the adducts shows a slight ellipticity that indicates an increment or decrement of electronic density, compared with isolated CO, in a preferred direction; (c) In 1 the major axes of the O-Mg and C-O bond ellipticities are parallel (the bonds are conjugated) while in 2 the major axes of the ellipticities of the C-Mg and C-O bonds are perpendicular to one another and the bonds are not conjugated; (d) It is shown [11] that the isolated CO molecule shows large accumulation of charge in the nonbonded regions of each atom, but the concentration is greater in the region corresponding to the oxygen atom.

The data indicate that in 1 the C-O-Mg bonds are conjugated and as a result of this, delocalization charge density is transferred from the C-O bond and from the nonbonded region of the oxygen atom to the O-Mg bond. In 2, the carbonyl and C-Mg bonds are not conjugated, less charge is present in the C-Mg bond than in the O-Mg bond of 1 and charge from the nonbonded region of the oxygen atom is instead transferred and accumulated in the C-O bond. The differences between both isomers can be explained as due mainly to the polarizing effect of the positively charged Mg atom and to the easily polarizable and extended nonbonded density in the oxygen atom.

Acknowledgment. The authors wish to thank Consejo Nacional de Investigaciones Cientificas y Tecnicas, R. Argentina and Comision de Investigaciones Cientificas de la Provincija de Buenos Aires, R. Argentina, for financial support and CESPI, UNLP for computational time.

References

1. Jubert A H, Maluendes SA, Castro EA, Nakamoto K: submitted
2. Klopman G (1968) J Am Chem Soc 90:223
3. Bader RFW, Nguyen-Dang TT, Tal Y (1981) Rep Prog Phys 44:893
4. Bader RFW, Nguyen-Dang TT (1981) Adv Quantum Chem 14:63
5. Bader RFW, Beddall PM (1972) J Chem Phys 56:3320; Bader RFW, Runtz GR, (1975) Mol Phys 30:117; Srebrenik S, Bader RFW (1975) J Chem Phys 63:3945; Srebrenik S, Bader RFW, Nguyen-Dang TT (1978) J Chem Phys 68:3667; Bader RFW (1980) J Chem Phys 73:2871
6. Bader RFW, Slee TS, Cremer D, Kraka E (1983) J Am Chem Soc 105:5061; Cremer D, Kraka E, Slee TS, Bader RFW, Lau CDH, Nguyen-Dang TT, MacDougall PJ (1983) J Am Chem Soc 105:5069; Bader RFW, Tang TH, Tal Y, Biegler-Konigi FW (1982) J Am Chem Soc 104:946
7. Bader RFW, Anderson SG, Duke AJ (1979) J Am Chem Soc 101:1389
8. Bader RFW, Preston HJ (1969) Int J Quantum Chem 3:327
9. Bader RFW, MacDougall PJ, Lau DH (1984) J Am Chem Soc 106:1594
10. Bader RFW, Essen H (1984) J Chem Phys 80:1943
11. Bader RFW, MacDougall PJ (1985) J Am Chem Soc 107:6788
12. Banister AJ, Durrant JA, Garell IB (1985) J Chem Soc Faraday Trans 2 81:1771